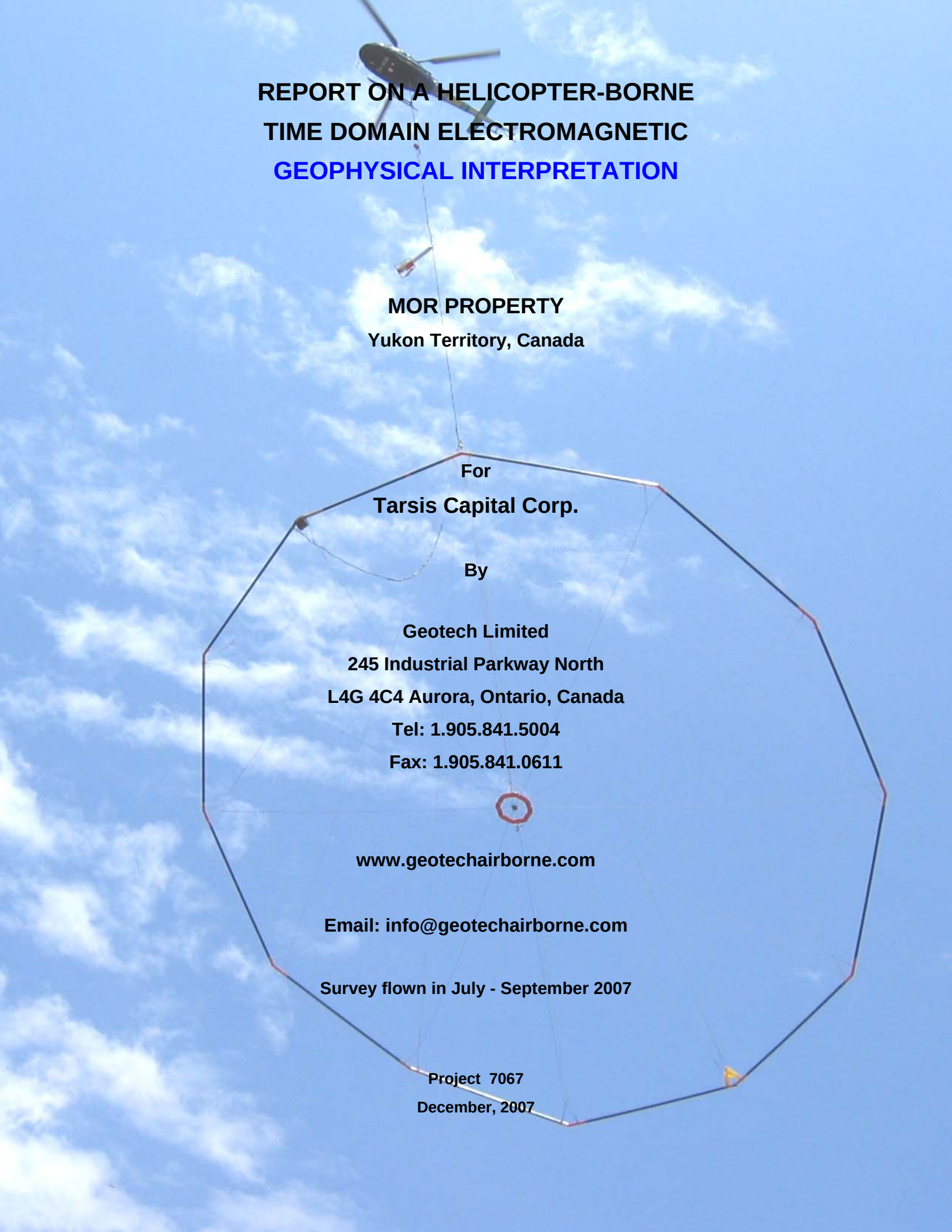

REPORT ON A HELICOPTER-BORNE TIME DOMAIN ELECTROMAGNETIC GEOPHYSICAL INTERPRETATION

MOR PROPERTY

Yukon Territory, Canada

For

Tarsis Capital Corp.

By

Geotech Limited

245 Industrial Parkway North

L4G 4C4 Aurora, Ontario, Canada

Tel: 1.905.841.5004

Fax: 1.905.841.0611

www.geotechairborne.com

Email: info@geotechairborne.com

Survey flown in July - September 2007

Project 7067

December, 2007

TABLE OF CONTENTS

1. INTRODUCTION.....3
2. SURVEY DESCRIPTION.....5
3. GEOLOGICAL CONSIDERATIONS.....6
3.1 Topography.....6
3.2 Regional geological context.....7
3.3 Geological context of the MOR Property.....8
3.4 Mineralization.....9
4. INTERPRETATION OF THE MAGNETIC DATA.....10
4.1 Introduction.....10
4.2 Analysis of the Magnetic data.....10
4.3 Inversion of the magnetic data.....15
5. INTERPRETATION of VTEM DATA.....17
5.1 Introduction.....17
5.2 VTEM anomalies shape.....17
5.3 Analysis of the EM results.....18
5.4 Selected Anomalies.....25
5.5 Conductivity Depth Sections.....25
6. CONCLUSIONS AND RECOMMANDATIONS.....30
7. REFERENCES.....31

Appendix A: VTEM Anomaly Modelling……..….32

REPORT ON A HELICOPTER-BORNE
TIME DOMAIN ELECTROMAGNETIC INTERPRETATION

MOR Property, Yukon Territory, Canada

1. INTRODUCTION

In July and September, 2007 a helicopter-borne electromagnetic survey was carried out by Geotech Ltd. for Tarsis Capital Corp. over the MOR Property located in Yukon Territory, Canada.

This report includes the results of the geophysical interpretation, over this Property. The Property is located at approximately 180 km south-east from Whitehorse, in the Yukon Territory. The geographic coordinates of the block extents are: longitudes, 132º 09'21" W and 132º 02'48" W, and latitudes, 60º 03'02" N and 60º 05'42" N. The surveyed area is 28 km^2, and the total line kilometers flown are 305 km (Fig. 1).

The survey was conducted using Geotech Ltd VTEM system. Principal geophysical sensors included a versatile time domain electromagnetic system and a high resolution cesium magnetometer. Ancillary equipment included a GPS navigation system and a radar altimeter.

Data processing and map compilation, including generation of final digital data products were achieved at the office of Geotech Ltd in Aurora, Ontario.

The present report describes the results of the geophysical interpretation of this Property.

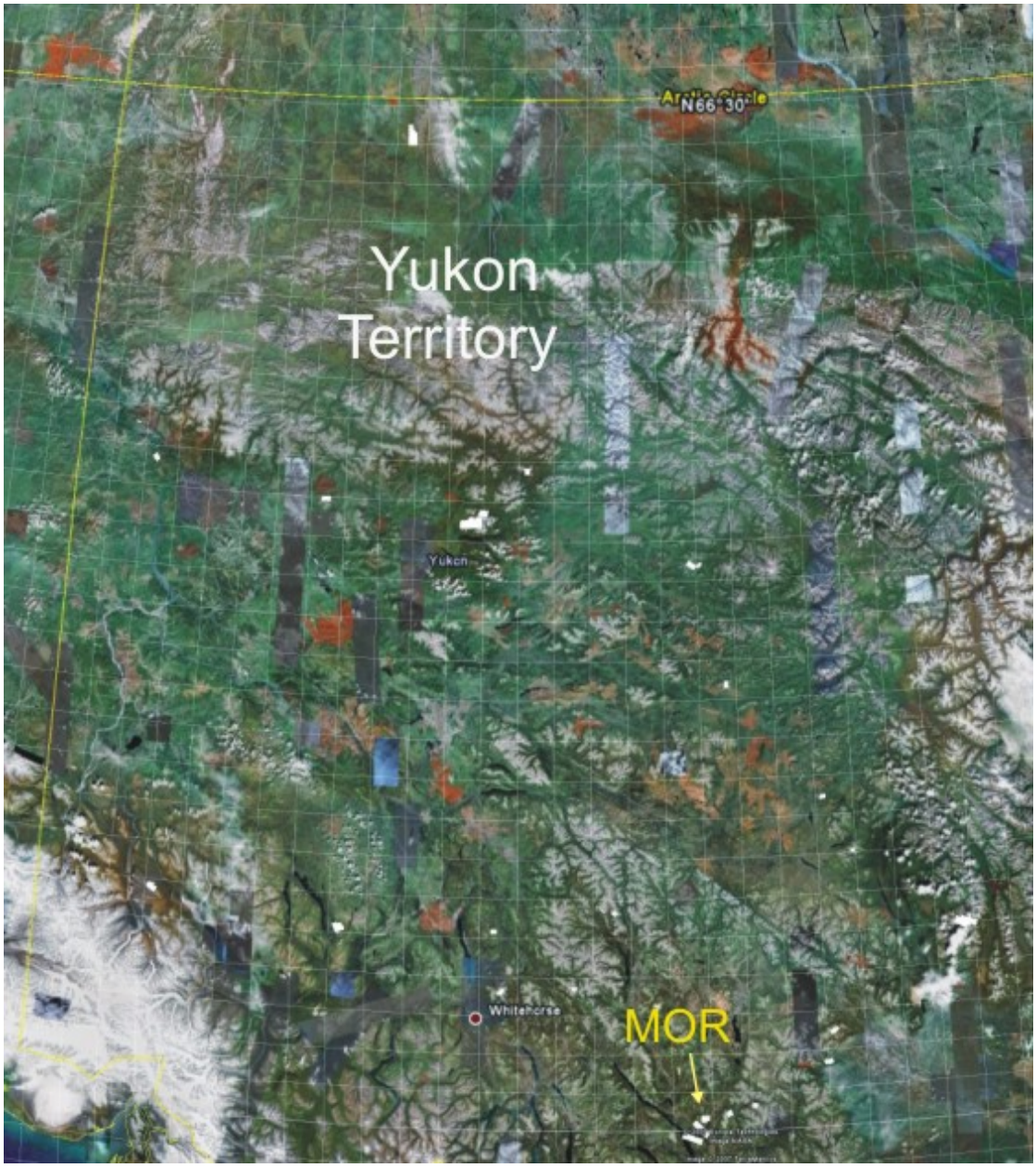

Fig. 1 Location of the MOR Property on the satellite image.

2. SURVEY DESCRIPTION

In July and September 2007, Geotech Ltd. carried out a helicopter-borne geophysical survey over the MOR property located in Yukon. Geotech Ltd. utilized a Versatile Time Domain Electromagnetic System to measure the electromagnetic induction field (B-field) and the vertical component of its time derivative (dB/dt). The electromagnetic measurements were made at the off-time mode. The concentric in-loop system was towed at a distance of 42 m from the helicopter. The VTEM Transmitter uses a trapezoid waveform shape with 7.2 ms duration operating at a base frequency of 30Hz. The dipole moment was approximately 425 000 NIA. The half-waveform was 16.7 ms.

A towed cesium and high resolution magnetometer was used to measure the Earth's magnetic field intensity. Data positioning and navigation were assured by a Novatel WAA GPS with accuracy less then 3 m.

A Terra TRA radar altimeter was used to measure the terrain clearance. The helicopter was flying at a constant speed of 80 km/h and was keeping a constant ground clearance of 85 m when the terrain allowed it. The traverse lines direction was NS and the tie lines direction was EW. The distance between the traverse lines and the tie lines was 100 m and 1000 m, respectively. A more detailed description of the survey parameters is provided in the logistics/processing report.

3. *GEOLOGICAL CONSIDERATIONS*

3.1 Topography

The terrain is very rugged with high mountain belts trending in the NS direction. The absolute altitude ranges from 800 m to 1500 m approximately. Due to the terrain roughness, it was difficult to keep a constant ground clearance while surveying this area.

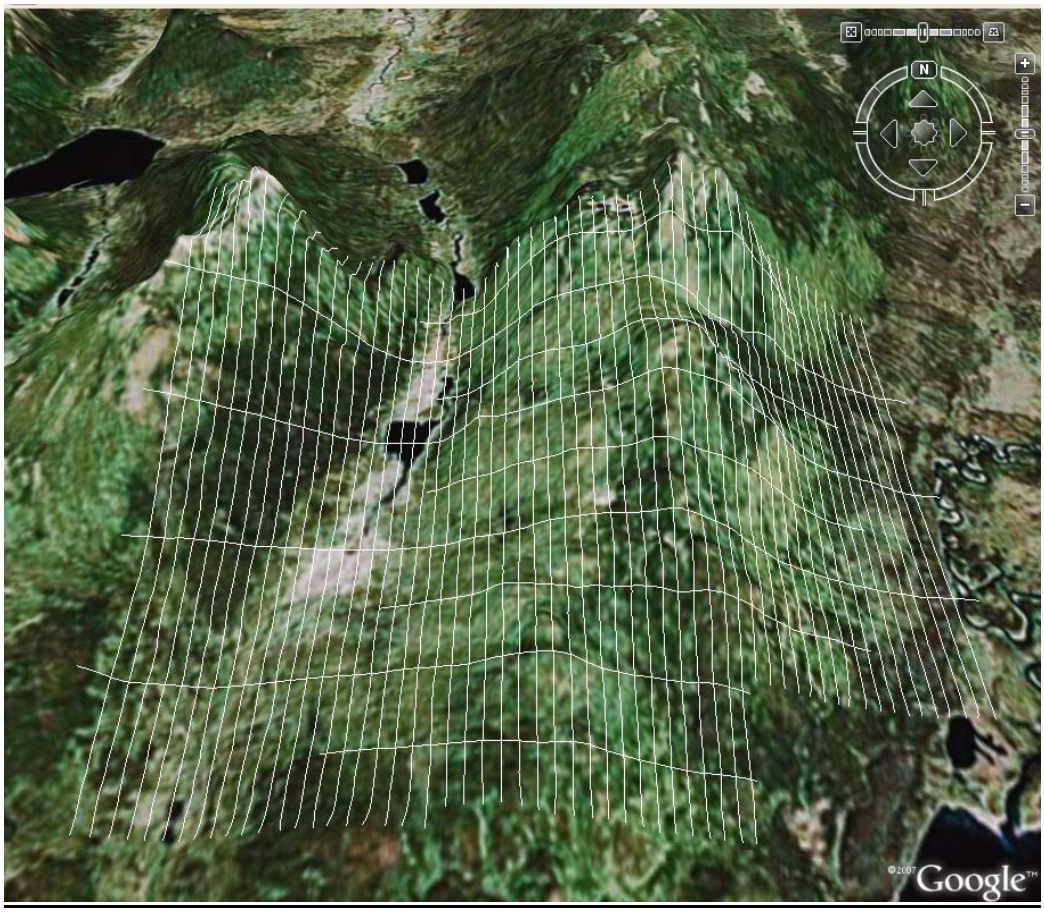

Fig.2 Topography of the MOR Property with the flight path.

3.2 Regional geological context

The Yukon Territory is situated in the northern part of the large geologic (and physiographic) belt known as the Cordillera. It is composed of relatively young mountain belts that range from Alaska to Mexico. The Yukon Territory is composed of a diverse type of rocks recording more than a billion years of geological history. Most of them have been affected by folding, faulting, metamorphism and uplift during various tectono-metamorphic events over at least the last 190 million years. This deformation has resulted in a complex arrangement of rock units and the mountainous terrain that has shaped today's geology. Geologically, Yukon is divided into two main components which are largely separated by the Tintina Trench. Formations northeast of the Tintina Fault consist of a thick, older sequence of sedimentary rocks which was deposited upon a stable geological basement. Rocks southwest of the Tintina Trench are composed of a younger, complex mosaic of igneous and metamorphic, representing numerous accreted terranes (Fig. 3).

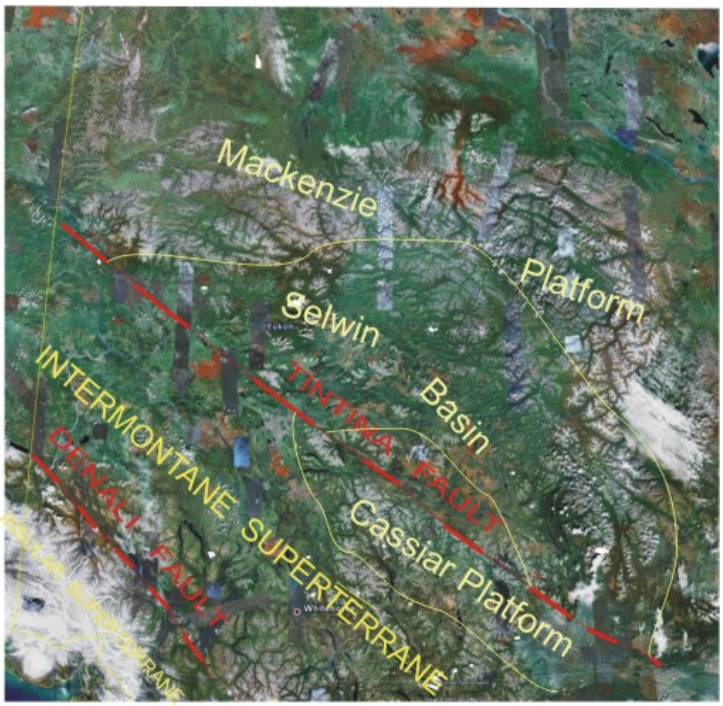

Fig.3. The major tectonic elements of Yukon superimposed on the satellite image. The figure indicates that the territory is composed of two dominant rock packages separated by the Tintina Fault: thick packages of sediments (northeast) and accreted Terranes (Southwest).

3.3 Geological context of the MOR Property

The MOR property is mostly underlain by a gently to moderately southward dipping sequence of quartz chlorite schist with mafic to intermediate volcanic/ volcanoclastic origin. These rocks are strongly deformed and easterly trending dipping in the southern direction (Fig.4).

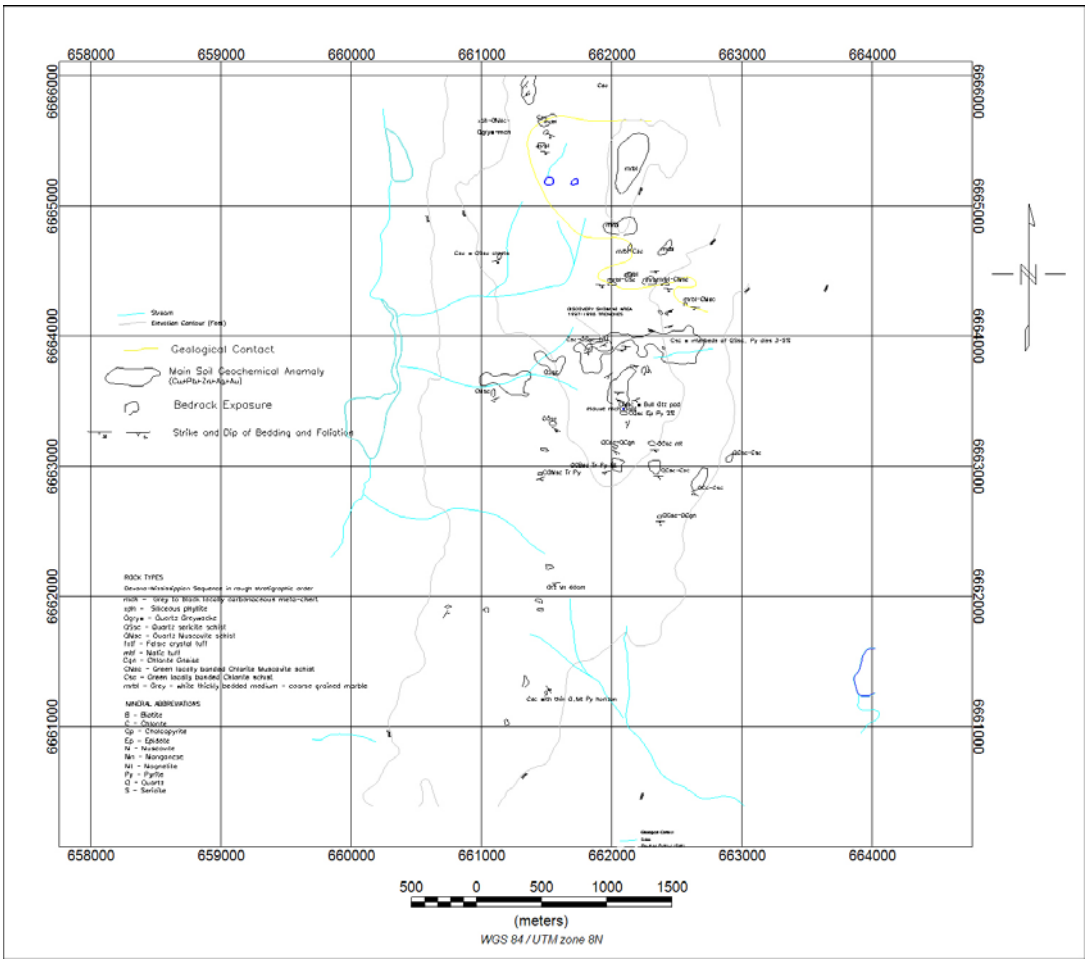

Fig. 4 Geological scheme of the MOR Property.

3.4 Mineralization

Disseminated, semi-massive and massive sulphide mineralization hosted within a cyclical mafic and felsic volcanic stratigraphic section, had been identified in this area. The sulphide mineralization is dominated by coarse pyrite with irregular accumulations of chalcopyrite and sphalerite.

During the year of 2004, drill holes located roughly 100 m apart tested a surface showing referred to as the "Discovery Horizon" exposed by previous hand and blast trenching. The position and projected trace of the Discovery Horizon is marked by a linear zinc-lead-copper soil geochemical anomaly outlined for some 2.5 km. A stronger area of copper, lead and silver response, located one kilometer south of the drill holes was not tested in 2004. Work in 2007 confirmed the interpreted gently dipping geometry of the Discovery Horizon tested the continuity of the mineralization down dip and laterally along strike.

4. INTERPRETATION OF THE MAGNETIC DATA

4.1 Introduction

Aeromagnetic surveys are routinely used as a powerful tool at different stages in mining exploration and in geological mapping. Because geological formations have different concentrations of magnetic minerals, they exhibit different magnetic signatures in the magnetic field, depending on the susceptibility contrast of rocks and the characteristics of the magnetic field. Thus, observed magnetic field over an area, can provide useful information that can assist the lithological and the structural mapping. It can be used to detect iron-rich mineral deposits, and/or mineral deposits associated with highly magnetic rocks (mafic and ultramafic formations).

4.2 Analysis of the Magnetic data

The observed magnetic field over the MOR Property is shown in Fig.5. The amplitude difference in the magnetic field intensity is approximately 300 nT. A large negative anomaly is observed in the eastern part of the area. This anomaly is related to non-magnetic metasediments existing in this area (schist and marble). Elsewhere, the area is dominated by positive anomalies with different shape. A banding anomaly composed of short wavelength lineaments trending in the NW direction is clearly indicated in the TMI map. Another system of magnetic lineaments with a NE direction is observed. The indicated lineaments are probably associated with mafic dykes and/or faults with magnetite contents.

Figure 6 shows the reduced to the pole magnetic field map, upward continued to 100m. The RTP map does not differ too much from the original map; however it better highlights the NW trending banding anomaly.

Since the contents of the observed magnetic maps include the response of shallow and deep magnetic sources, it is difficult to analyze the maps containing various wavelength anomalies. Distinguishing shallow features from deeper ones can be performed via several methods of field separation and filtering. The Fig. 7 illustrates the vertical gradient of the TMI. The vertical gradient map shows the enhancement of magnetic signals caused by shallow sources and related to faults and contacts. The tilt derivative map illustrated in Fig. 8 yields another example of amplifying weak signals generated by shallow sources. The tilt derivative known as being the local phase is computed from the vertical and horizontal gradients. As illustrated in the Tilt derivative map several shallow magnetic structures can be identified in this area. Most of them are probably associated with faults or hidden mafic dykes.

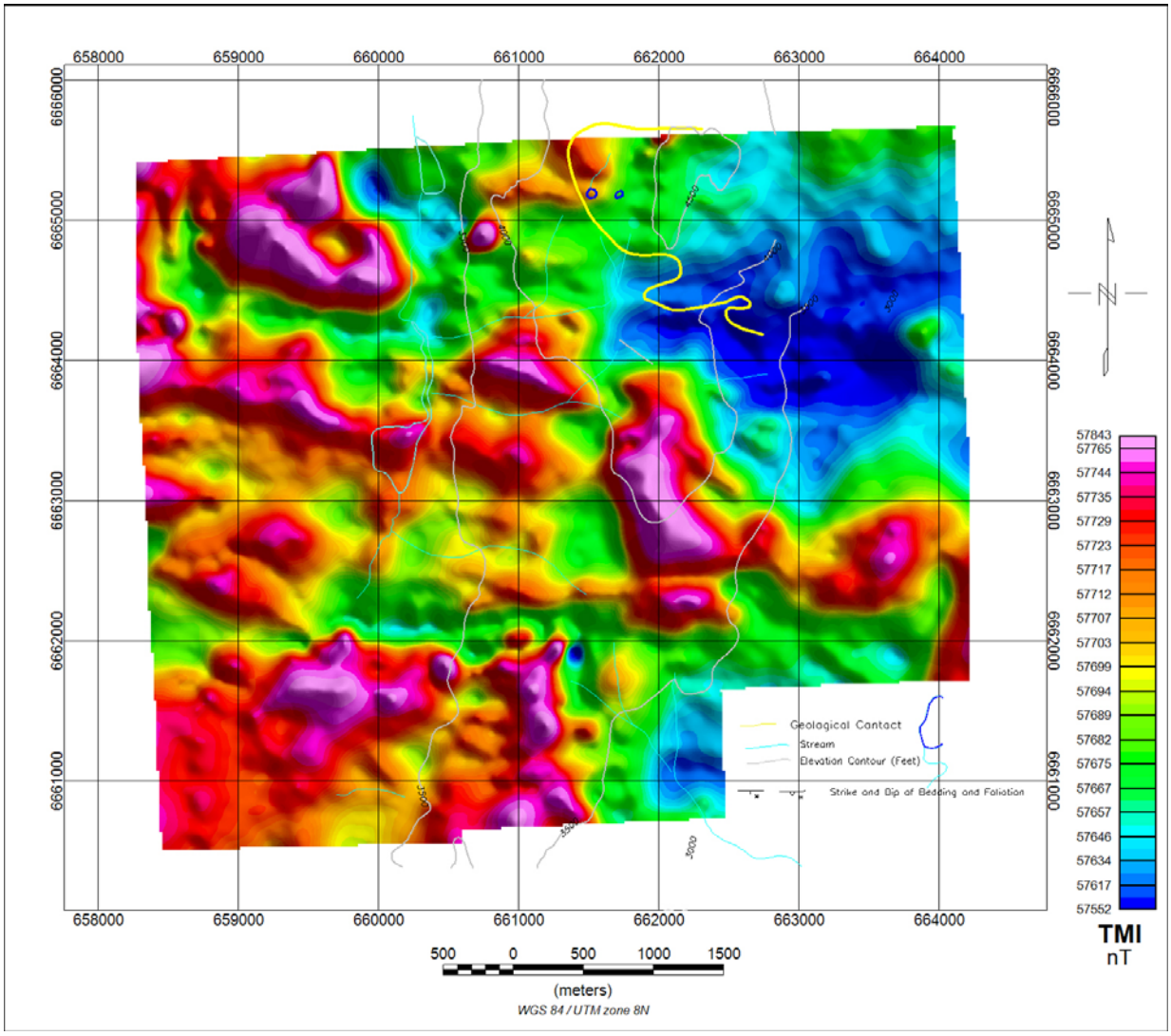

Fig. 5 TMI image of the MOR Property.

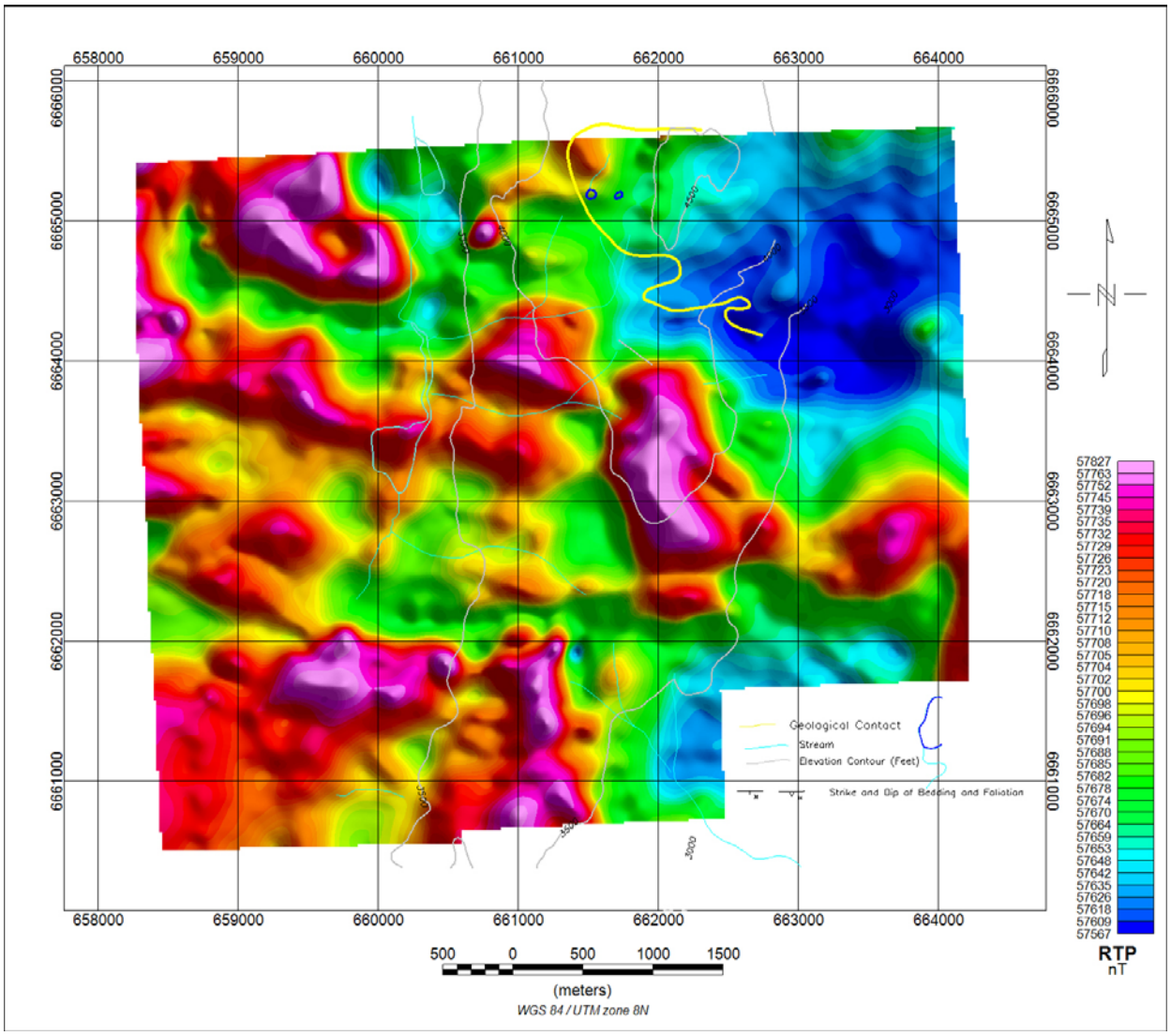

Fig.6 Color shaded relief of reduced to the pole TMI.

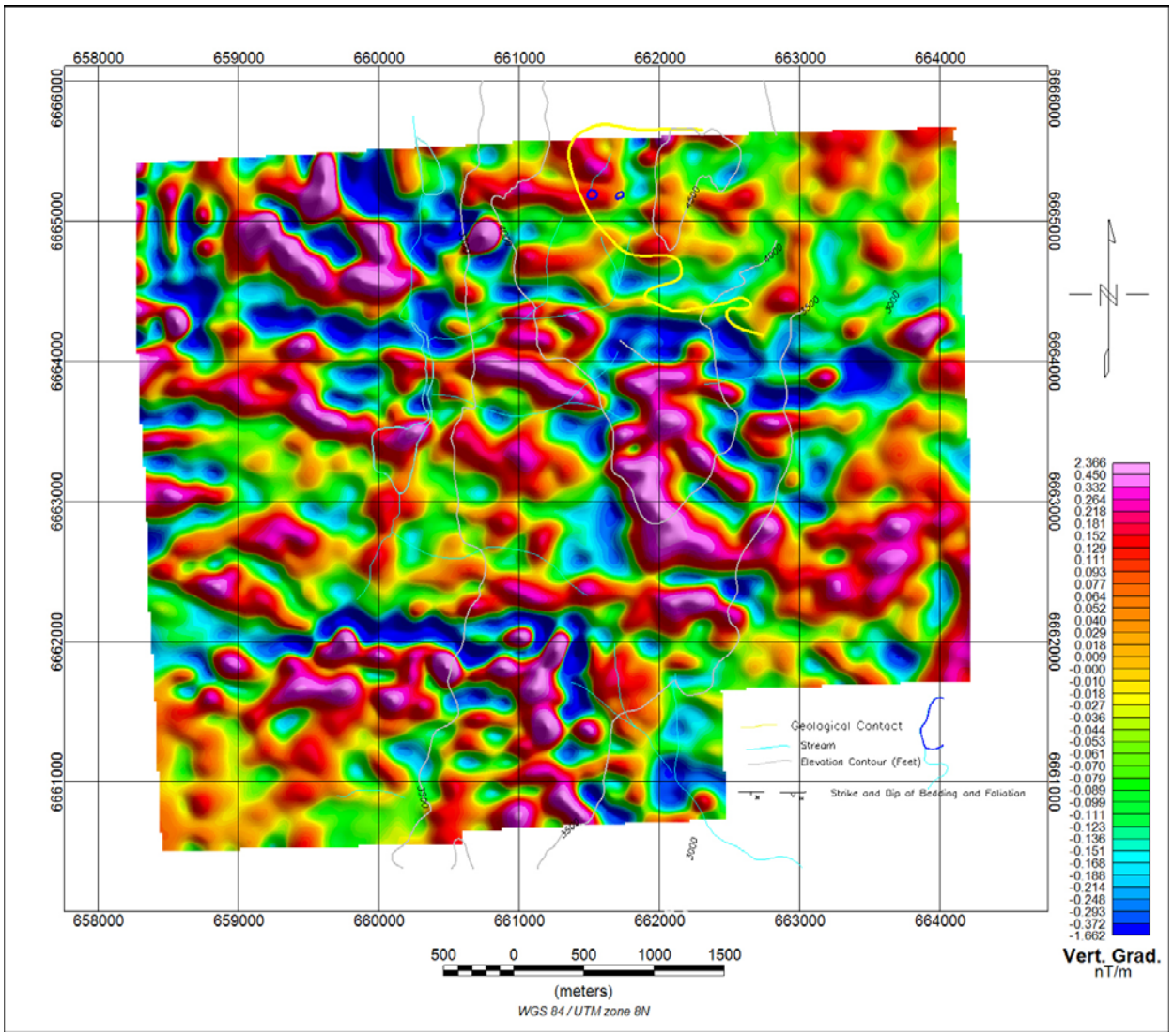

Fig.7 Color shaded relief of the vertical gradient of the magnetic field.

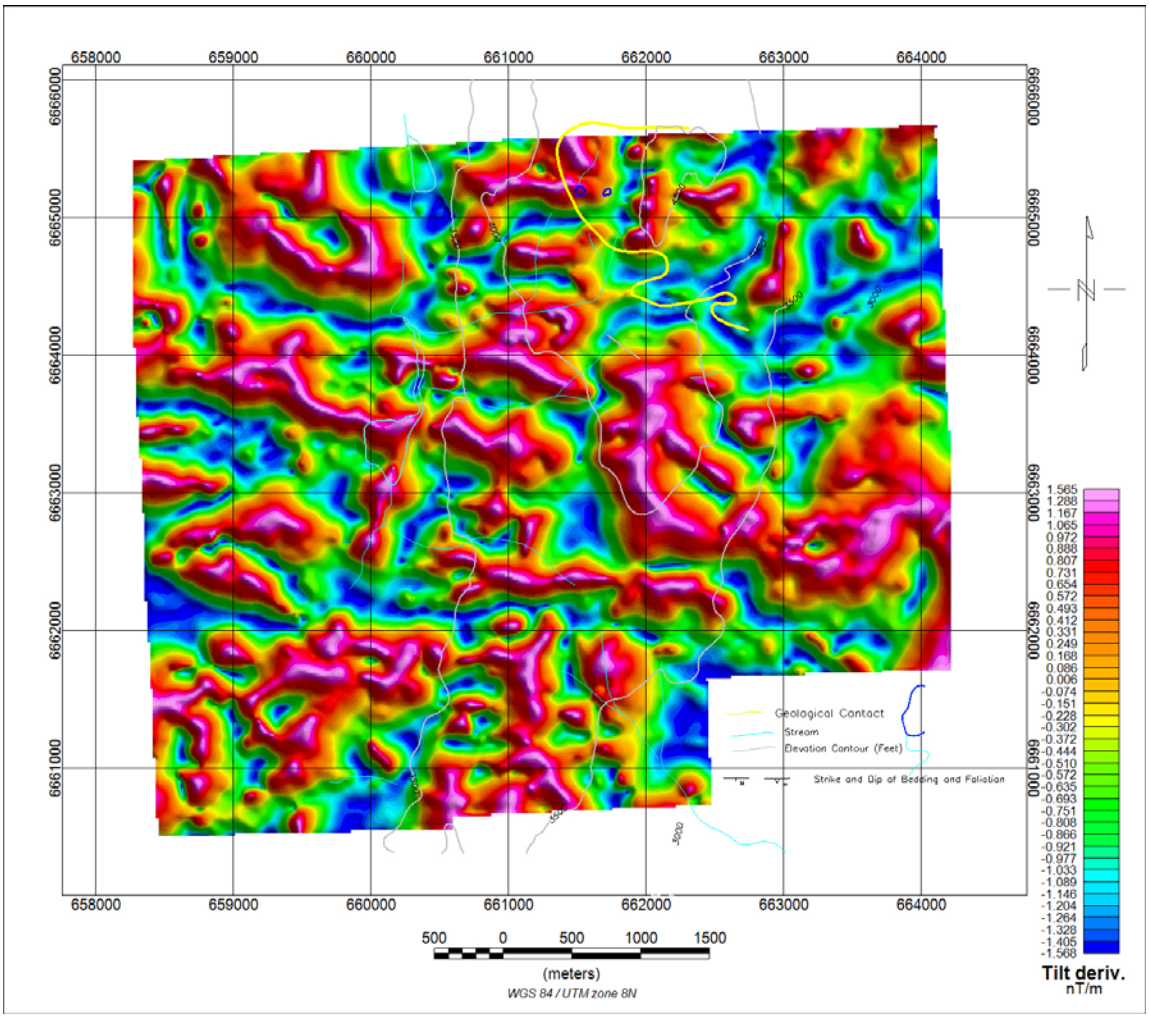

Fig. 8 Color shaded relief of the Tilt derivative.

4.3 Inversion of the magnetic data

Several computer-based techniques can be used to automatically detect magnetic sources and yield estimations of their geometrical and physical parameters. These techniques can be either used to gridded data (3D methods) or to profiles (2D methods). Euler deconvolution is a well established technique, allowing a rapid interpretation of a large amount of magnetic data. This method is mainly aimed to delineate magnetic sources boundaries and to estimate their depths.
Fig. 9 shows the results obtained with the Euler deconvolution inversion using a structural index of 1, a depth tolerance of 10% and a square deconvolution window having a size of 400 × 400 metres. Euler solutions have been plotted on the total gradient (analytic signal) map for better illustration. The picks of the total gradient are used to located and delineate the magnetic sources boundaries. Euler solutions are mostly related to shallow sources (<100 m). Most of them are related to linear magnetic structures tending in the NW. Results obtained with the Euler deconvolution confirm the qualitative analysis of the reduced maps. Another lineament trending in the EW direction has also been identified and confirmed in the southwestern part of the area.

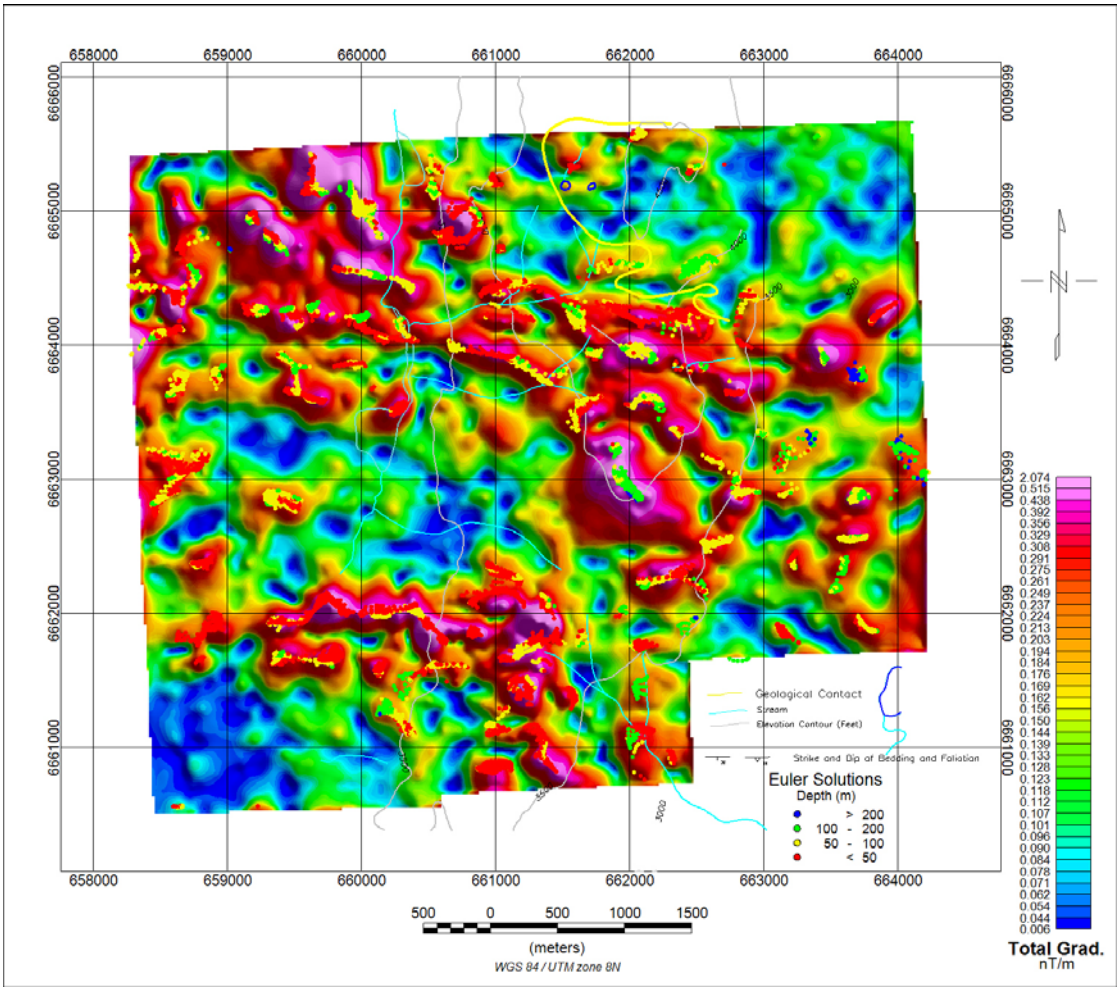

Fig. 9 Euler deconvolution solutions plotted on the total gradient image.

5. INTERPRETATION of VTEM DATA

5.1 Introduction

Transient electromagnetic surveys have proven to be a very efficient tool in mineral exploration by detecting hidden deposits characterized by higher conductivities than the medium in which they are embedded. Because Time domain systems have a much greater depth penetration compared to the Frequency domain systems, these systems are considered as a tool of choice in the mining exploration. The Geotech Helicopter VTEM system, operating in the Time domain, uses concentric-loop geometry with the receiver mounted in the centre of a larger transmitter loop. Both loops are oriented in the vertical plane. This configuration has a number of advantages, as a maximum coupling, sharper anomalies by comparison to airborne fixed wing systems, and the shape of the anomalies in independent of the flight path orientation. Furthermore, the high moment transmitter combined with the lower terrain clearance yields stronger secondary field signals in most conductors when compared to other systems. The actual VTEM systems measure both the electromagnetic induction field B and its time derivative dB/dt. This system specificity has a lot of advantages, as the dB/dt better resolves the shallow conductive sources while the B-field exhibits a better resolution for deep conductors.

5.2 VTEM anomalies shape

For concentric-loop geometry systems when both loops are oriented in the Z-axis (VTEM system) thick dipping or horizontal conductors exhibit a characteristic single peak, while steeply dipping and thin conductors manifest a double peak. The minimum indicates the location of the top of the thin conductor, and the major peak indicates the side towards which the conductor is dipping. Synthetic models anomalies were generated for the plate type conductors are provided in the Appendix A to better understand the shape of the VTEM anomalies

5.3 Analysis of the EM results

Figures 12 and 13 show the stacked profiles in pseudo-logarithmic scale of the dB/dt and B-field channels, respectively. Both maps show the existence of 4 anomalous zones (A, B, C, and D). Zone B, located in the southern part of the area contains the strongest anomalies (Fig. 11). Zones A, C, and D are characterized by weaker EM response, however the observed anomalies in these zones exhibit negative late time decays. The cause of the existence of negative decays at late time is explained by the polarization effect that is commonly observed over electrically polarizable areas containing metallic disseminated minerals. Fig. 10 shows the EM decays above the Discovery Showing area with heavily disseminated sulfide mineralization (pyrite and chalcopyrite).

The interpretation of the EM profiles was performed using in-house built software for automatically picking the anomalies along the profiles and yielding estimates of the conductance and the decay constant (tau) of isolated anomalies. The picked EM anomalies were posted on the late time EM channel. Figures 14 and 15 illustrate the results of the picked anomalies superimposed on the dB/dt, and B-field late time channel (3.911 ms after shut off), respectively.

The interpretation indicates the presence of poor linear conductors in the central and southern parts of the map and trending in the east-western direction. The estimated conductance values do not exceed 5 ms except for the anomalous zone B, where one value of 12 S was obtained. The estimated decay constants are low (less than 3 ms) except for the anomalous zone B, where higher decay constants where obtained.

It is worth mentioning that the observed EM anomalies are in very good spatial correlation with the observed magnetic signal (Fig. 16).

The interpretation map (Fig. 17) shows the results of the magnetic and electromagnetic analysis superimposed on the magnetic total gradient image. The magnetic interpretation suggests the existence of two cross cutting faulting systems trending in the NW and in NE, respectively. It also shows that the detected EM anomalies are in very good correlation with magnetic and VLF signals. The anomalies detected in the southern area (Zone B) are probably related to deep conductive bedrock containing a possible massive sulfide mineralization. However, the anomalies detected in the northern part of the block (A, C, and D) are more likely to be associated with a shallow poor conductor containing disseminated sulfide mineralization.

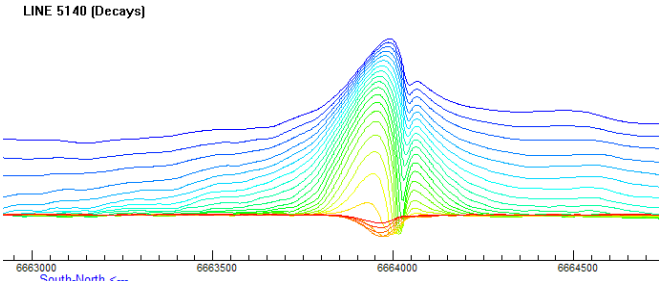

Fig. 10 EM profiles showing positive early time, and negative late time decays over the Discovery Showing area. Zone C, Line 5140.

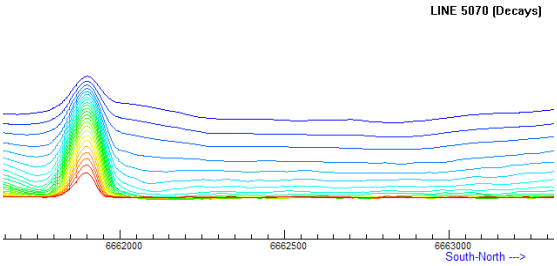

Fig. 11 EM profiles showing positive decays over the anomalous Zone B, Line 5070.

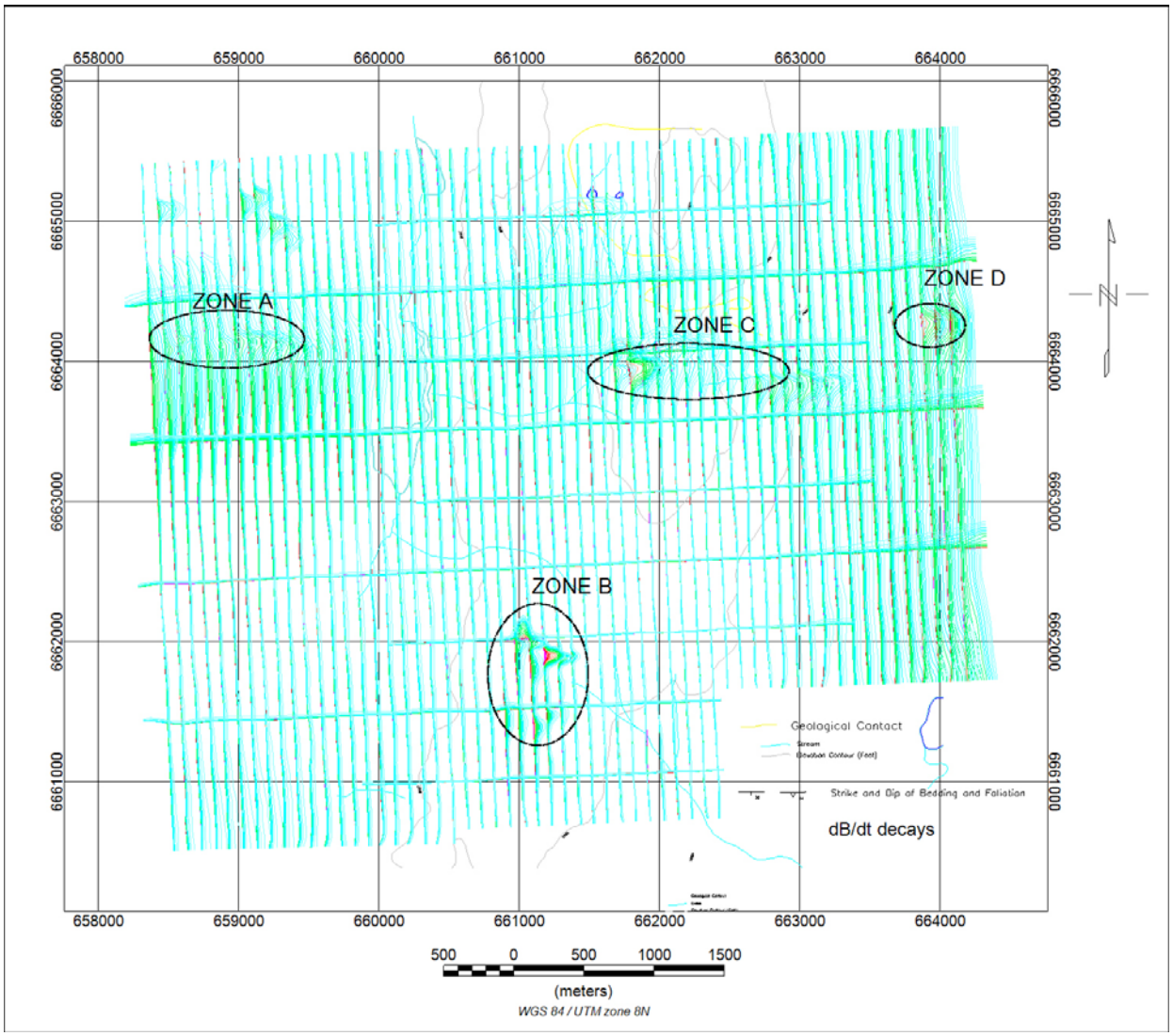

Fig. 12 Stacked EM dB/dt profiles at log-linear scale. Early time decays are in green and late time in red.

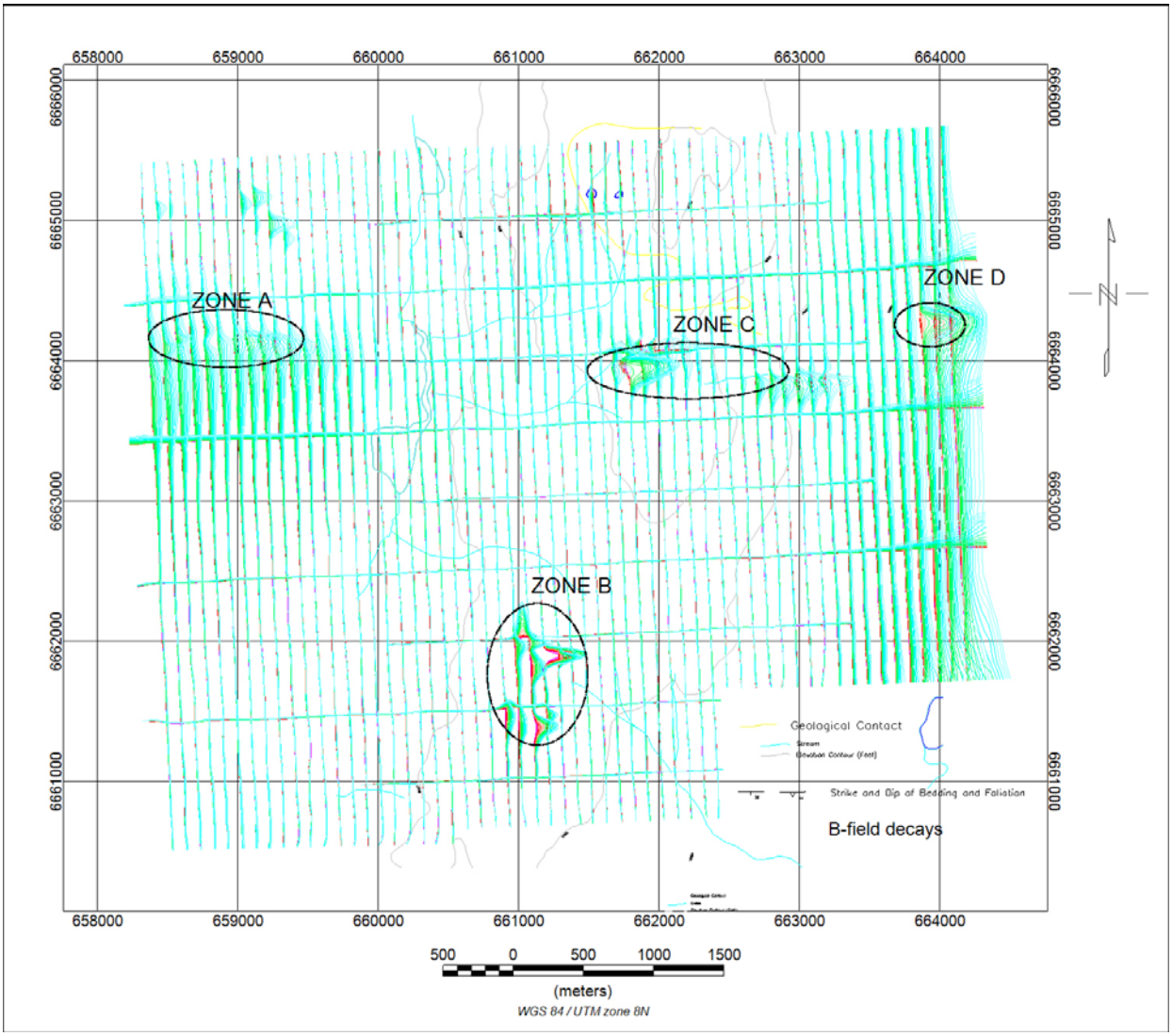

Fig. 13 Stacked EM B-Field profiles at log-linear scale. Early time decays are in green and late time in red.

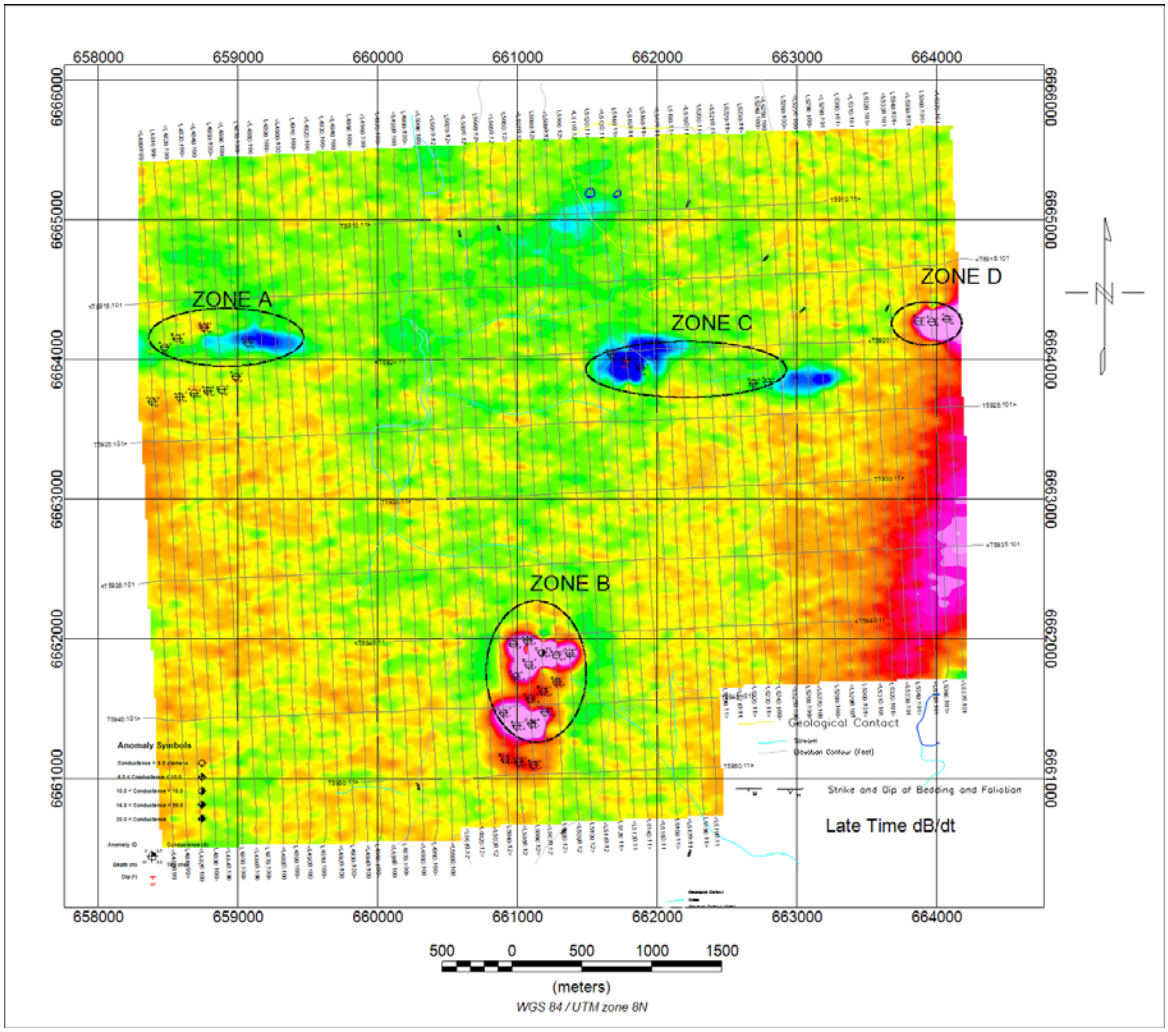

Fig. 14 EM picked anomalies plotted on the late time dB/dt channel image. Negative anomalies are indicated in blue, positive, in red and purple.

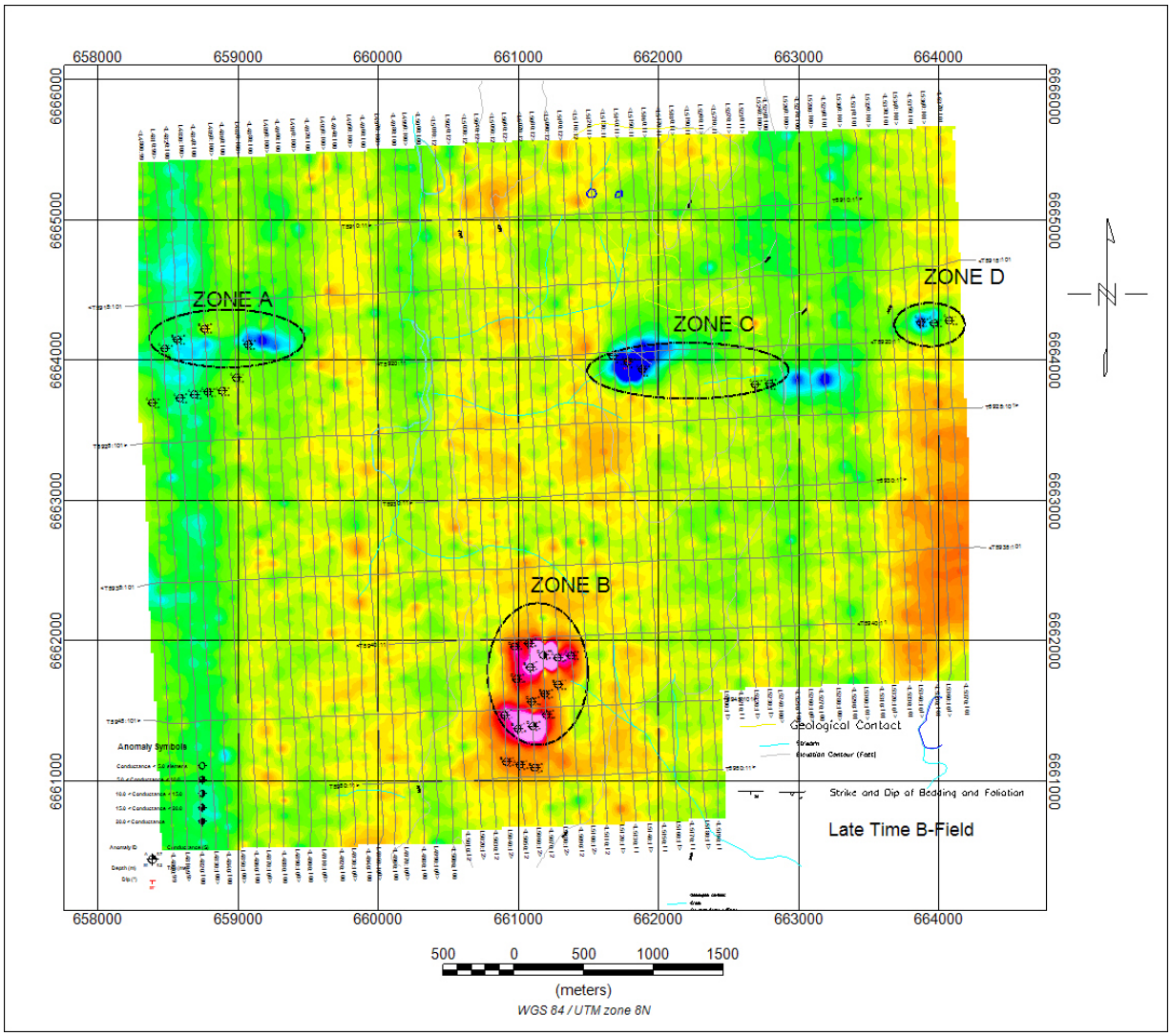

Fig. 15 EM picked anomalies plotted on the late time B-Field channel image. Negative anomalies are indicated in blue, positive, in red and purple.

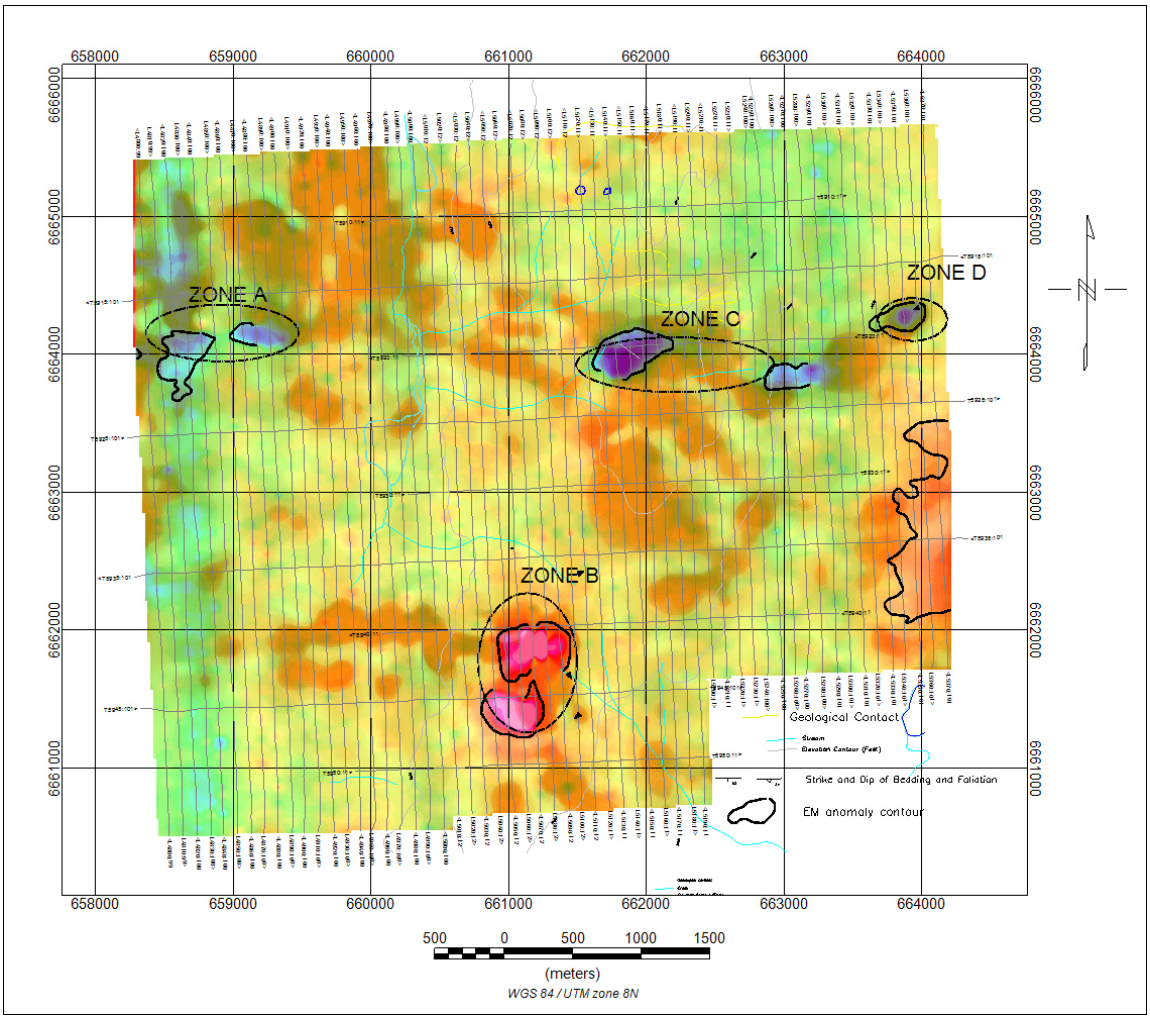

Fig. 16 Late time B-Field channel image superimposed on the magnetic total gradient. The dark spots indicate high values of the total gradient. The map shows a very good correlation of the EM anomalies with the magnetic signal.

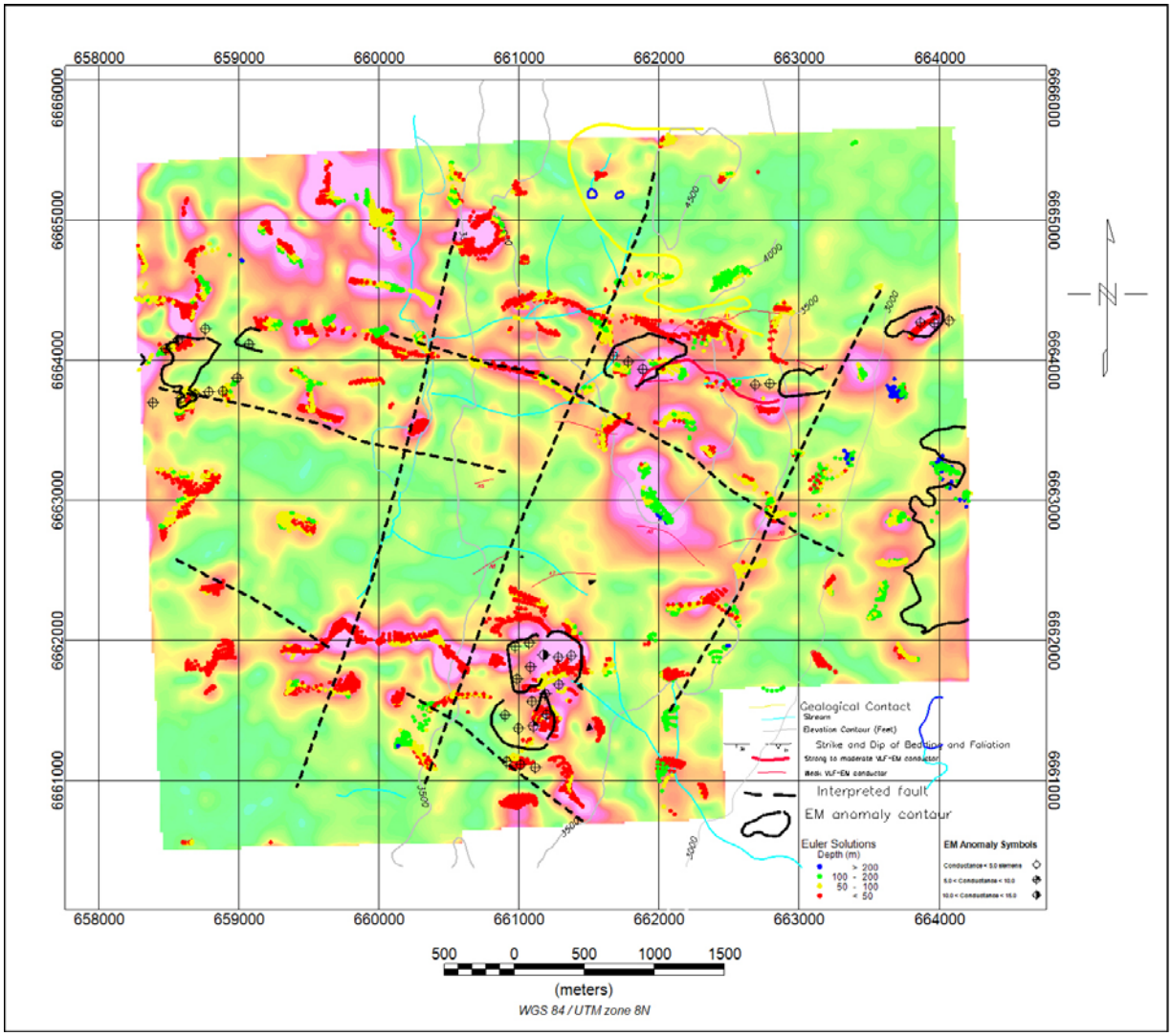

Fig. 17 Interpretation map showing the results of the magnetic and electromagnetic data analysis.

5.4 Selected Anomalies

Four individual anomalies extracted from the described above anomalous zones have been selected for modeling by converting the EM decays into CDIs. The anomalies are located on the following lines: L4840, L5070, L5140, and L5360. The summarized characteristics of the selected anomalies are given in the following table:

Line	Anomaly ID	Anomaly Type description	Conductor geometry	X- location m	Y- location m	Conductance S	Dip	Dip Azimut	Tau msec
L4840	B	One broad anti-symmetric peak	Thick shallow dipping plate	658758	6664225	3		S	3.6
L5070	C	One symmetric peak	Thick steeply dipping plate	661175	6661898	12			3.9
L5140	A	Double peak anti-symmetric	Thin shallow dipping plate	661778	6663992	2.7	24°	SW	0.2
L5360	B	One broad anti-symmetric peak	Thick shallow dipping plate	663964	6664266	4.4		S	0.5

Table 1. Summarized results of the selected anomalies.

5.5 Conductivity Depth Sections

Conductivity depth imaging is considered as one of the important steps in the analysis and interpretation of electromagnetic data. CDI allows providing useful information of the conductivity distribution of the considered cross section. CDI were performed for the selected lines using the EMflow software. The obtained results are shown in Figures18-21.

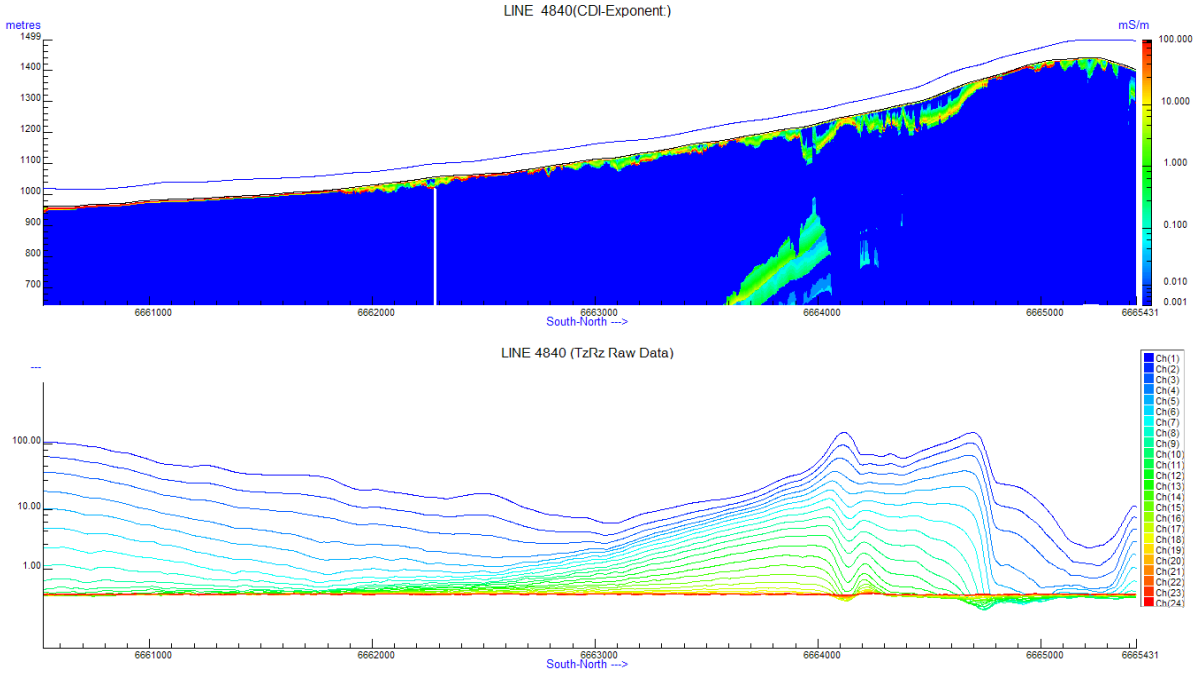

Figure18 shows the CDI section for the line L4840. The section indicates the presence of a poor conductor at a depth more than 200 m dipping in the southern direction.

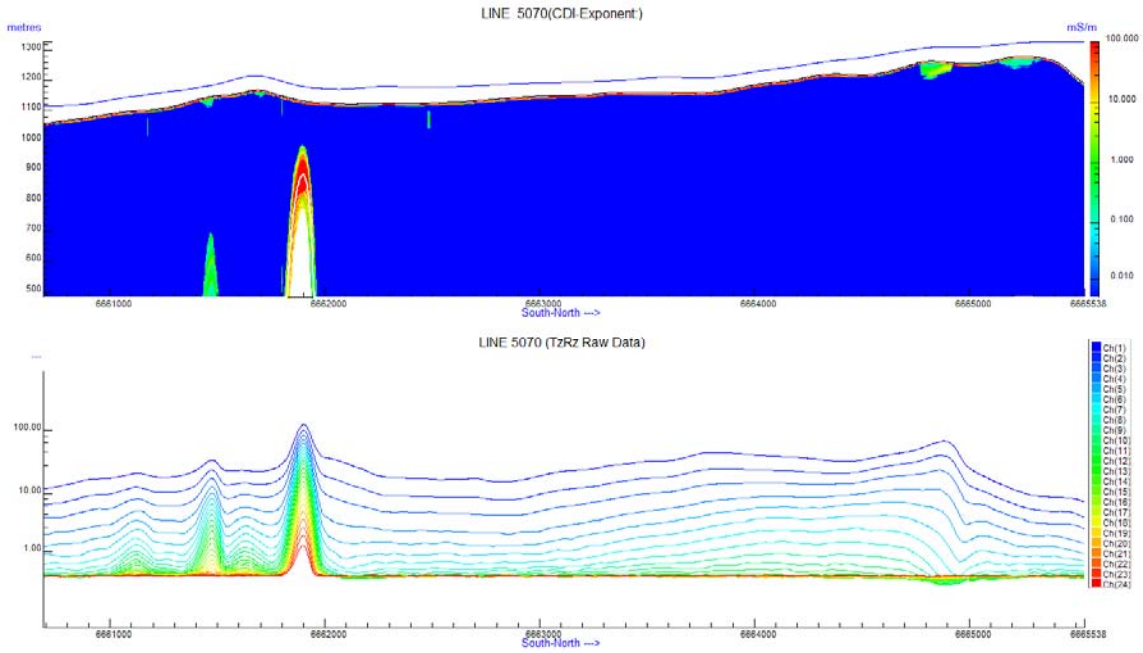

Figure 19 shows the CDI section for the line L5070. The section indicates the existence of good conductive bedrock at the approximate depth of 150m. A possible massive sulfide mineralization is associated with the conductive body.

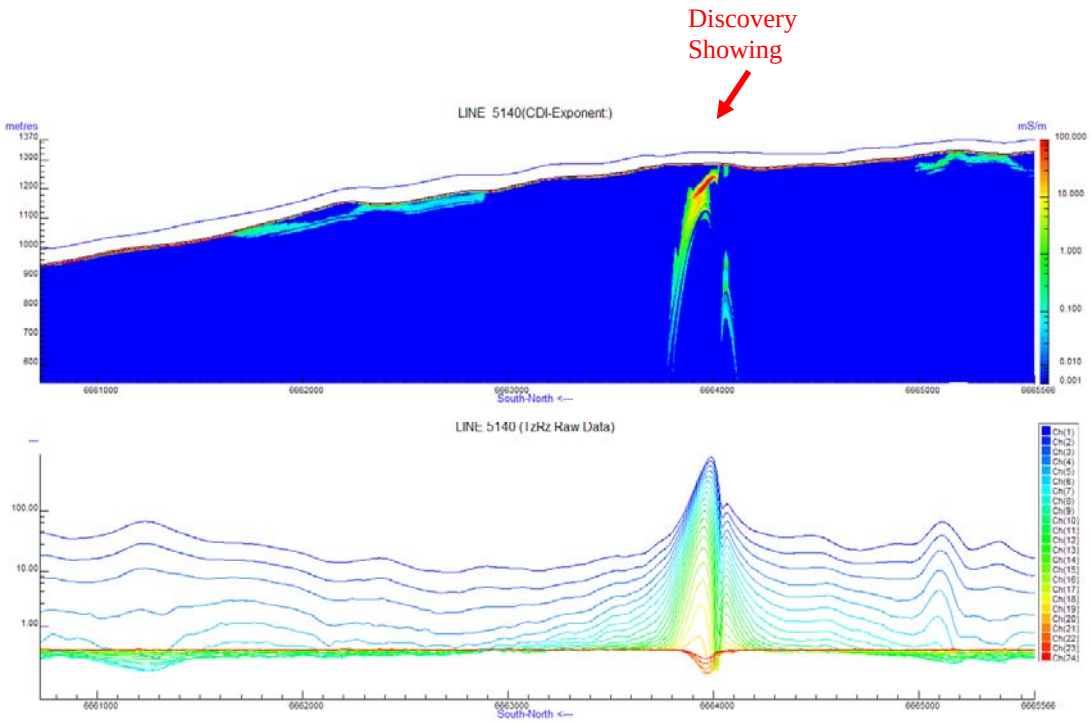

Figure 20 shows the CDI section for the line L5140. The section highlights the existence of surfacial shallow dipping thin conductor. It also shows that the conductor has a limited depth extension. The anomy is observed over the Discovery showing with disseminated sulfide mineralization.

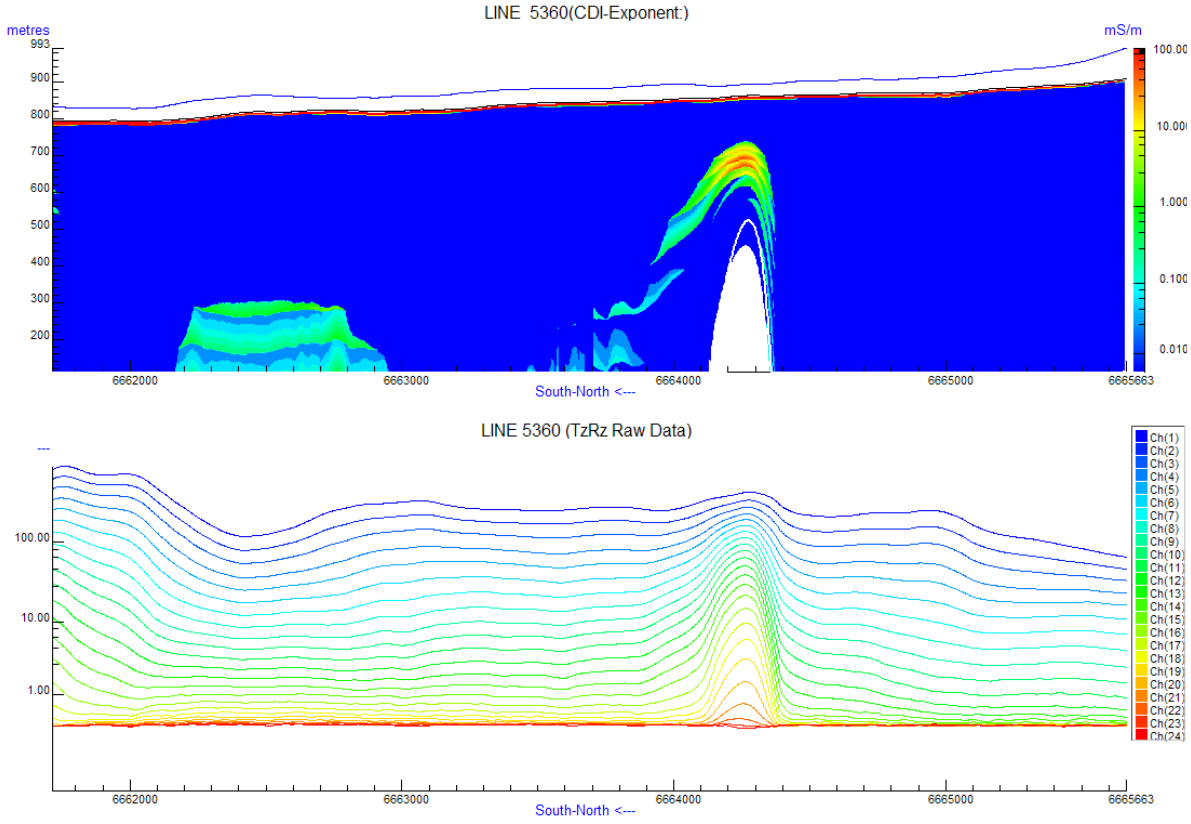

Figure 21 shows the CDI section for the line 5360 (Anomalous Zone D). The section shows the existence of a southerly dipping poor conductor.

6. CONCLUSIONS AND RECOMMANDATIONS

The analysis of the magnetic map of the MOR property revealed the existence of several lineaments related to shallow structures. The Euler deconvolution inversion method has shown that most of the detected magnetic sources are situated at depth less than100 m. The magnetic interpretation using different reduced maps suggests the presence of a two cross cutting faulting systems trending in the NNW and NNE directions.

The VTEM survey reveals the existence of 4 anomalous zones in very good correlation with the magnetic filed and VLF signal as well (Zone C). Three zones situated in the northern part are trending more or less in the east west direction and are related to highly disseminated sulfide mineralization. The detected anomalous zone in the southern part (Zone B) is associated with conductive bedrock suggesting the possible presence of massive sulfide mineralization at an approximate depth of 150 m.

The recommendation is to conduct some drilling tests on the anomalous zone B (Line L5070), which is possibly related to massive sulfide mineralization.

Respectfully submitted,

Dr. Nasreddine Bournas
Geotech Ltd.
December, 2007

7. REFERENCES

1. J. CHEN, A. RAICHE, AND J. MACNAE, 2000, Inversion of airborne EM data using thin-plate models, SEG 2000 expanded abstracts.

2. STOLZ, E.M.G. AND MACNAE, J.C., 1991 Evaluating EM waveforms by singular-value decomposition of exponential functions. Geophysics, 63, 64-74

3. A.B. REID, J.M. ALLSOP, H. GRANSER, A.J. MILLETT AND I.W. SOMERTON, 1990, Magnetic interpretation in three dimensions using Euler deconvolution, , G*eophysics, 55, 80-91*.

4. Yukon Geological Survey, www.geology.gov.yk.ca

APPENDIX A

VTEM ANOMALY MODELING

I. THIN PLATE

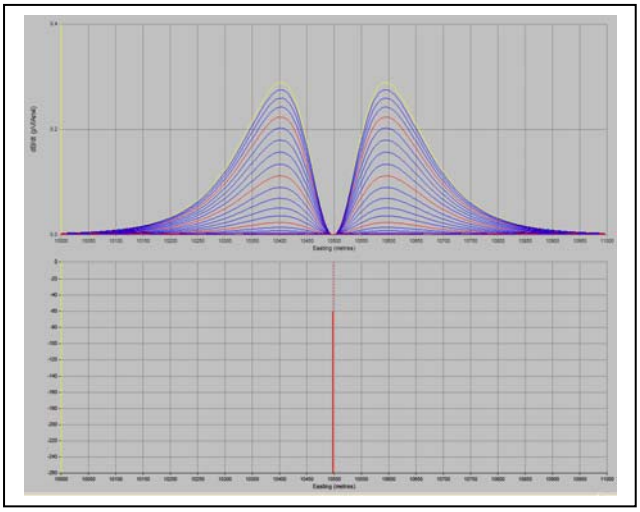

Figure A-1: dB/dt response of a shallow vertical thin plate. Depth=100 m, CT=20 S. The EM response is normalized by the dipole moment and the Rx area.

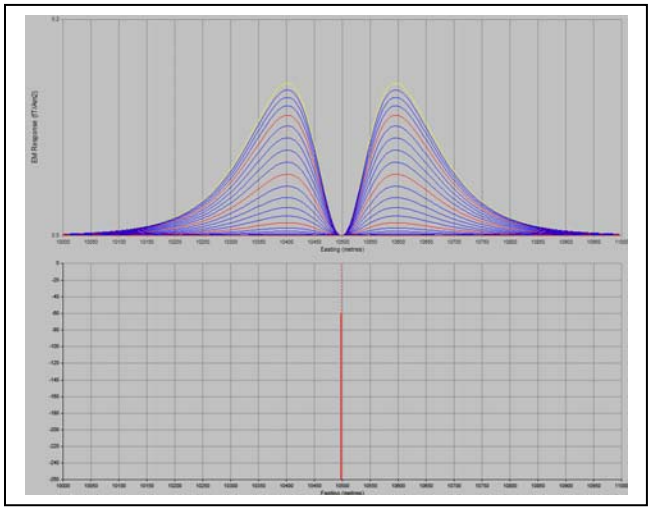

Figure A-2: B-field response of a shallow vertical thin plate. Depth=100 m, CT=20 S. The EM response is normalized by the dipole moment.

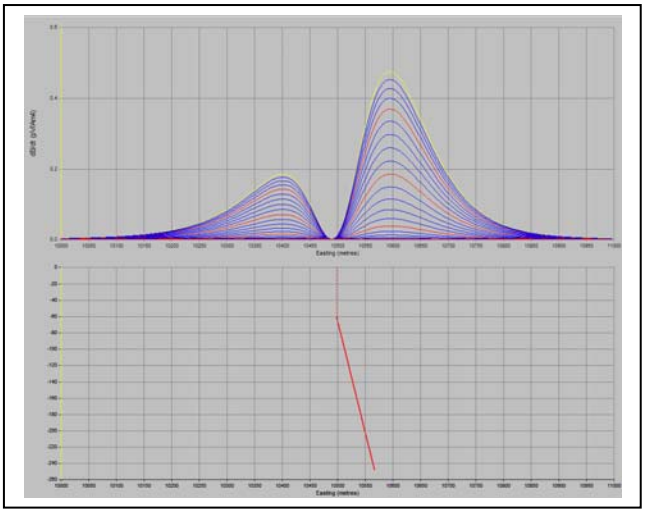

Figure A-3: dB/dt response of a shallow skewed thin plate. Depth=200 m, CT=20 S. The EM response is normalized by the dipole moment and the Rx area.

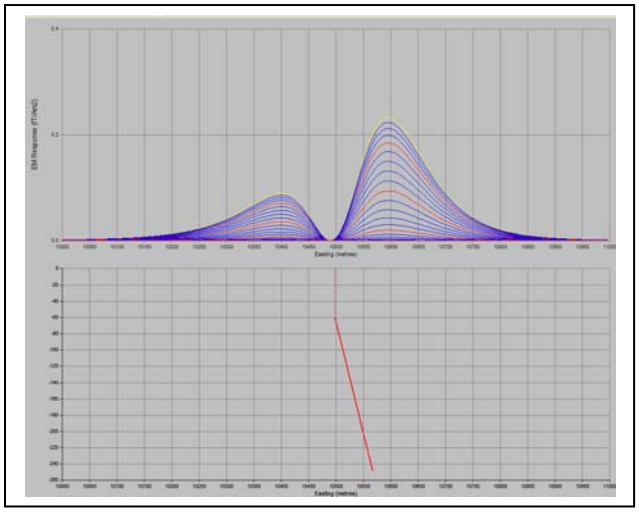

Figure A-4: B-field response of a shallow skewed thin plate. Depth=100 m, CT=20 S.The EM response is normalized by the dipole moment.

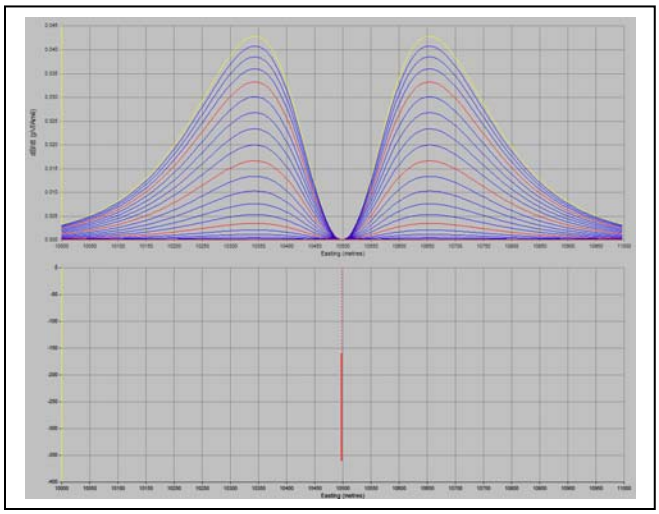

Figure A-5: dB/dt response of a deep vertical thin plate. Depth=200 m, CT=20 S. The EM response is normalized by the dipole moment and the Rx area.

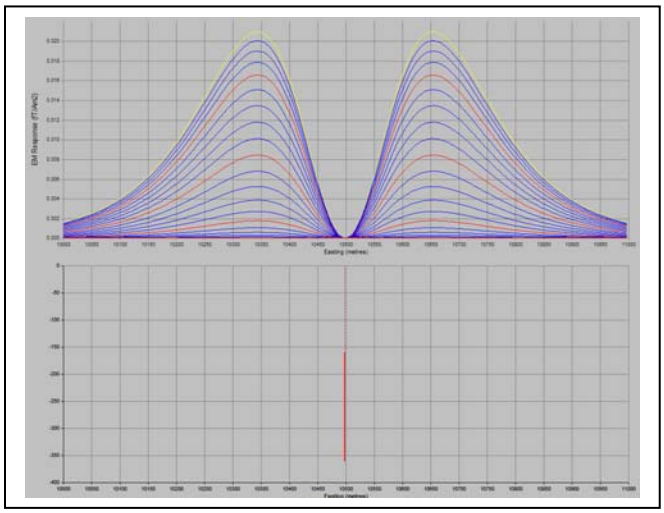

Figure A-6: B-Field response of a deep vertical thin plate. Depth=200 m, CT=20 S. The EM response is normalized by the dipole moment.

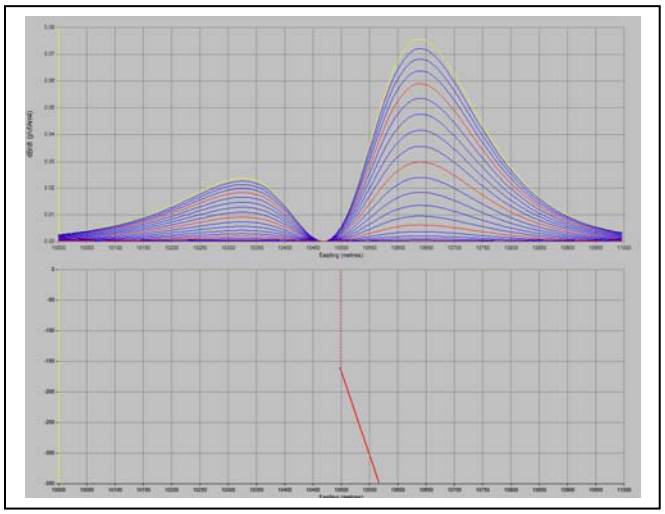

Figure A-7: dB/dt response of a deep skewed thin plate. Depth=200 m, CT=20 S. The EM response is normalized by the dipole moment and the Rx area.

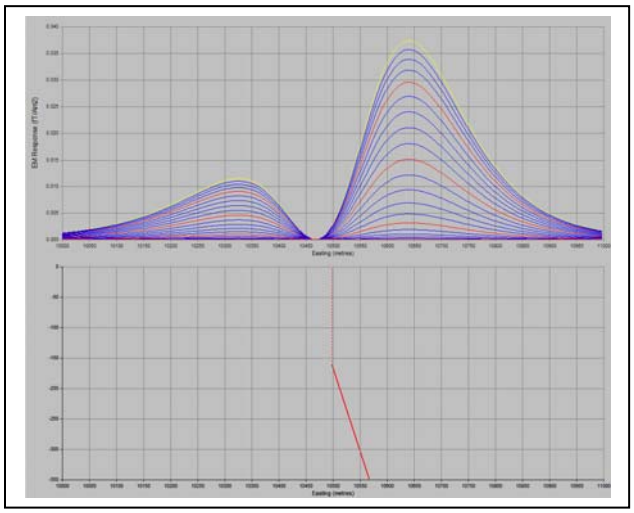

Figure A-8: B-field response of a deep skewed thin plate. Depth=200 m, CT=20 S. The EM response is normalized by the dipole moment.

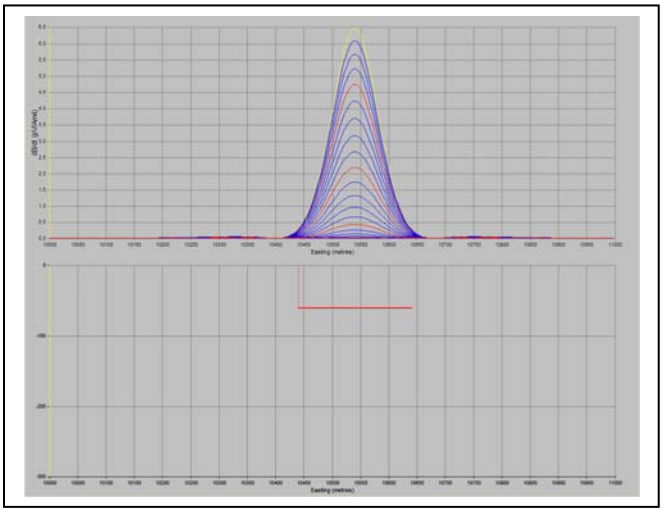

Figure A-9: dB/dt response of a shallow horizontal thin plate. Depth=100 m, CT=20 S. The EM response is normalized by the dipole moment and the Rx area.

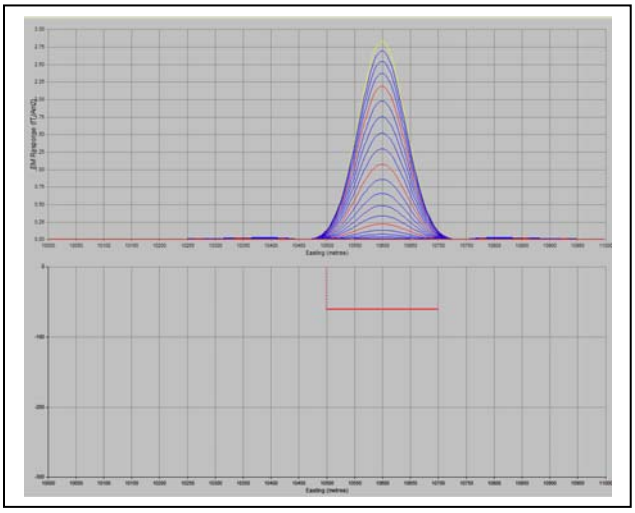

Figure A-10: B-Field response of a shallow horizontal thin plate. Depth=100 m, CT=20 S. The EM response is normalized by the dipole moment.

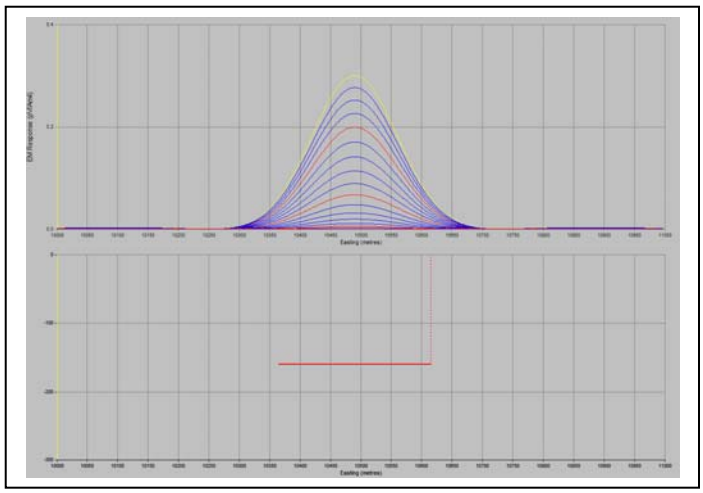

Figure A-11: dB/dt response of a deep horizontal thin plate. Depth=200 m, CT=20 S. The EM response is normalized by the dipole moment and the Rx area.

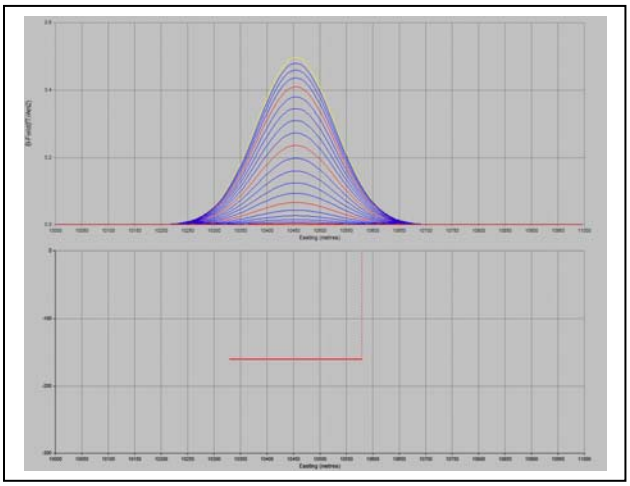

Figure A-12: B-Field response of a deep horizontal thin plate. Depth=200 m, CT=20 S. The EM response is normalized by the dipole moment.

II. THICK PLATE

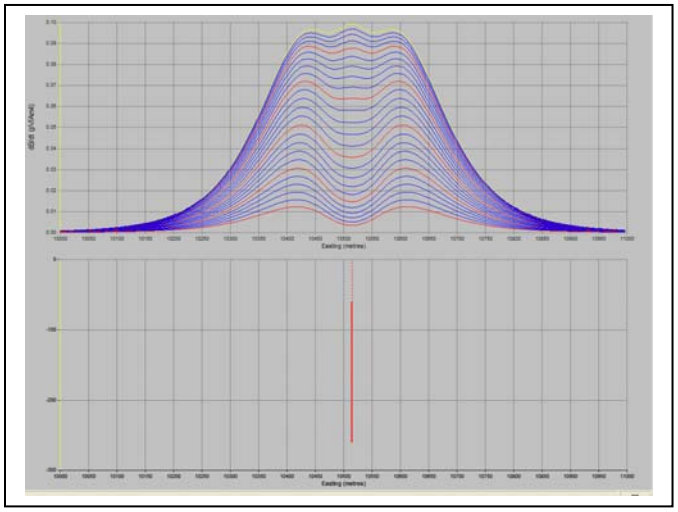

Figure A-13: dB/dt response of a shallow vertical thick plate. Depth=100 m, C=12 S/m, thickness=20 m. The EM response is normalized by the dipole moment and the Rx area.

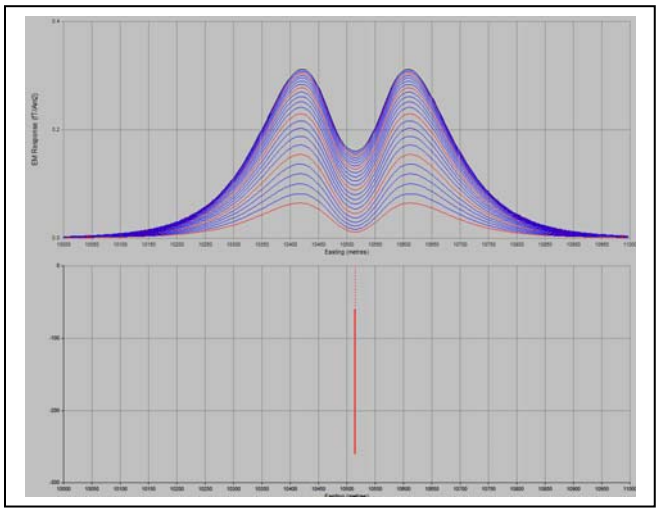

Figure A-14: B-Field response of a shallow vertical thick plate. Depth=100 m, C=12 S/m, thickness= 20 m. The EM response is normalized by the dipole moment.

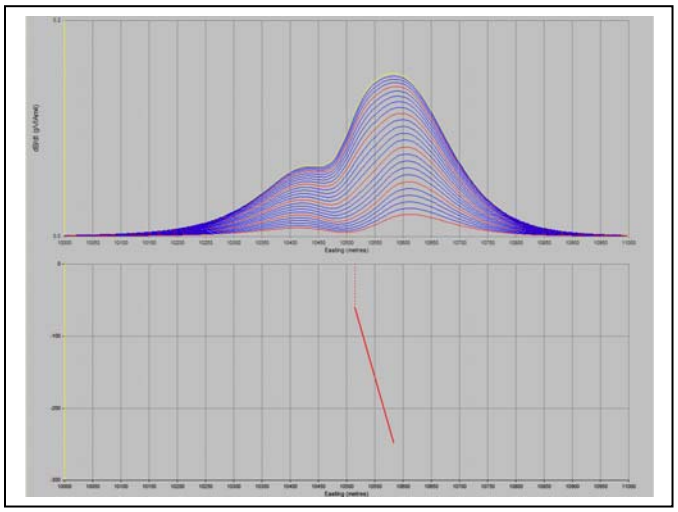

Figure A-15: dB/dt response of a shallow skewed thick plate. Depth=100 m, C=12 S/m, thickness=20 m. The EM response is normalized by the dipole moment and the Rx area.

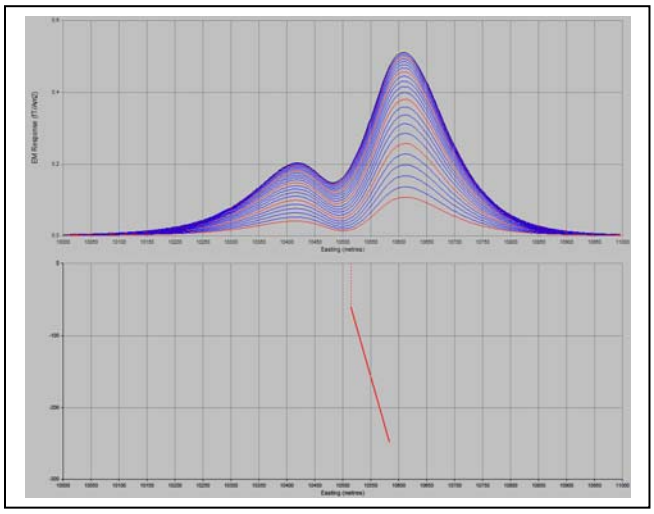

Figure A-16: B-Field response of a shallow skewed thick plate. Depth=100 m, C=12 S/m, thickness=20 m. The EM response is normalized by the dipole moment.

III. MULTIPLE THIN PLATES

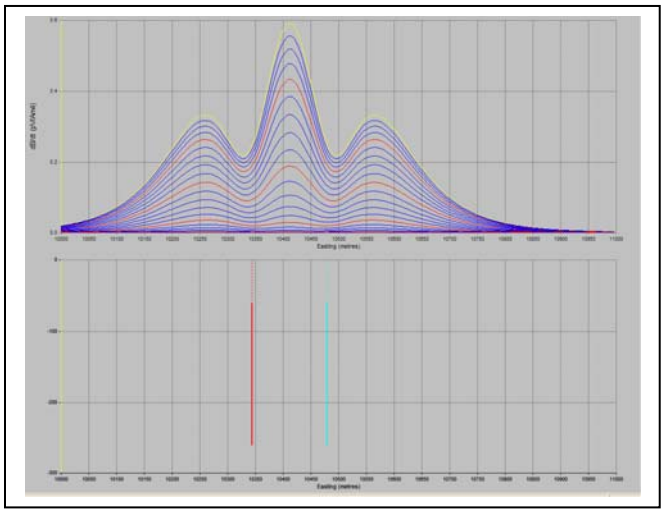

Figure A-17: dB/dt response of two vertical thin plates. Depth=100 m, CT=20 S. The EM response is normalized by the dipole moment and the Rx area.

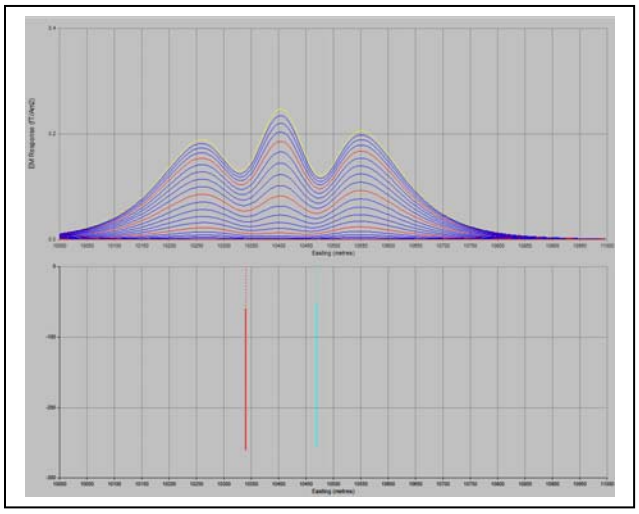

Figure A-18: B-Field response of two vertical thin plates. Depth=100 m, CT=20 S. The EM response is normalized by the dipole moment.